

IMPLEMENTATION OF MODELS FOR STRESS-REDUCED OXIDATION
INTO 2-D SIMULATOR

Albert Seidl¹, Veronika Huber², Evelyn Lorenz³

¹ Institut für Festkörpertechnologie, Munich, Germany

² Siemens AG, Munich, Germany

³ Arbeitsgruppe für Integrierte Schaltungen, Erlangen, Germany

1. SUMMARY

It has been shown by previous work [3,5] that models for stress-retarded-oxidation (SRO) are necessary to achieve realistic results when simulating local oxidation processes in two dimensions. In this work mathematical problems arising during the implementation of nonlinear models [1,6] for SRO into a 2-D numerical simulator are discussed. Due to stability problems a straightforward extension of Chin's procedure [2] was not possible. The significance of stress-effects is demonstrated by a comparison of simulation results with experimentally obtained oxide-profiles.

2. ACCURACY OF FINITE ELEMENT METHODS

In this work the 2-D simulator was realized by using the finite element method [7,8]. The numerical error of stress calculation using this method will be discussed. When interested in theoretical considerations on the accuracy of finite element methods the reader is referred to [4]. The elastic beam problem shown by Fig.1 was calculated with different grids. The displacement was measured at C and the peak values of tensile stress were measured at A and B. Tab.t1 shows the results for different grids calculated with linear shape functions. The values shown in Tab.2 were calculated on the basis of quadratic shape functions. It can be seen that in the case of linear shape-functions an accuracy of 0.1% is obtained only for a large number of grid-points, whereas the same accuracy can be reached for quadratic shape-functions with relatively coarse grids. The values of

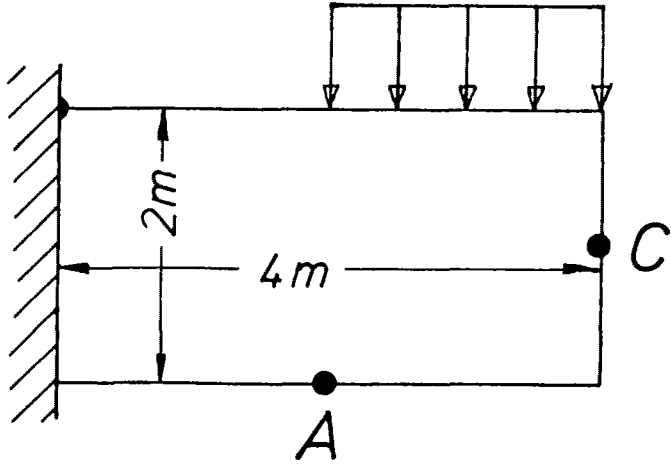


Fig.1: Geomtry of problem for finite element patch test

normal stress calculated as mean-values over the elements are very inaccurate independent from the order of the shape-function. It seems that even the finest meshes used within this test are too coarse to provide a proper representation of the stress-distribution.

Grid	d_c [mm]	σ_{nB}	σ_{nA} [kN/mm ²]
3x5	0.336	477	132
5x9	0.478	826	221
9x17	0.544	1067	275
17x33	0.565	1246	297
33x65	0.571	1420	304
65x129	0.572	1605	307

Tab.1: Test-results calculated with linear shape-functions

Grid	d_c	σ_{nB}	σ_{nA} [kN/mm ²]
2x3	0.562	227	108
3x5	0.568	554	179
5x9	0.571	798	236
9x17	0.572	982	272
17x33	0.572	1147	291
33x65	0.572	1315	301

Tab.2: Test-results calculated with quadratic shape-functions

3. THE MODELS FOR STRESS-RETARDED OXIDATION

3.1. Existence of solution for Kao's model

The stress dependence of the coefficients governing reaction, oxygen diffusion and oxide deformation is given by the following equations [6],[1]

- (1) $k_s = k_o \exp(-\sigma_n V_k/kT)$
- (2) $D = D_o \exp(-p V_D/kT)$
- (3) $C^* = C^*_o \exp(-p V_C/kT)$
- (4) $\mu = \mu_o \exp(p V_\mu/kT)$

where k_s denotes the reaction rate, D the diffusion coefficient of the oxidant in SiO_2 , C^* the saturation concentration, μ the viscosity, σ_n the normal stress along the Si-SiO₂ interface and p the hydrostatic pressure. V_k , V_D , V_C and V_μ are called activation volumes [1]. Normalized coefficients are introduced.

$$\begin{aligned} k_n &:= k_s C^*/N = k_1 \\ D_n &:= D C^*/N = k_p/2 \\ C_s &:= C_1/C^* \end{aligned}$$

where N denotes the number of oxidant molecules per unit volume. The gas phase transport coefficient is not taken into account under the assumption that $h \gg k_s$. For easier understanding and notation without loss of generality the rotational symmetric

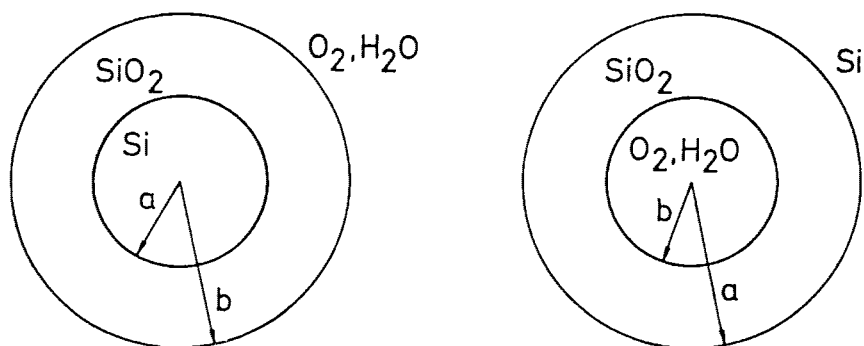


Fig.2: Geometry of rotational symmetric structure. right=concave, left=convex

case (s. Fig.2) [1] is now used for studying the consistence of the model equations when stress-dependent coefficients according to Eqs.(1), (4) are used. The ordinary initial value problem to be solved is given by

$$(5) \quad \frac{\delta a}{\delta t} = sg k_n C_s \alpha := sg R(a)$$

where $\alpha=0.44$ denotes the ratio of silicon consumed during oxidation/produced volume of oxide and sg is a sign-variable which accounts for convex ($sg=-1$) and concave ($sg=1$) structures. The value of the oxidant concentration at the Si-SiO₂ interface C_s is given by [1] as function of the geometry and the stress-dependent coefficients. Now a new stress parameter s is introduced

$$(6) \quad s := 2 \mu a sg k_n C_s (1-\alpha)$$

so that the pressure p and the normal-stress become [1]:

$$(7) \quad p = s/b^2$$

$$(8) \quad \sigma_n = s(1/b^2 - 1/a^2)$$

The expressions for stress-dependent constants are now entered into Eq.(6). The worst case (very thin oxide) can easily be considered:

$$(9) \quad a \approx b \quad \text{and}$$

$$(10) \quad C_{s0} \approx 1$$

If Eqs.(1)...(4) and (7), (8) are entered into (6)

$$(11) \quad s = sg \frac{(1-a)}{a} a \mu_0 k_{n0} \cdot \exp\left[s \left(\frac{V_u - V_k - V_c}{b^2} + \frac{V_k}{a^2} \right) / kT \right]$$

is obtained. C_{s0} and k_{n0} denote the stress-free values of C_s and k_n respectively. In this context it should be mentioned that an equation of the form

$$x = c_1 \exp(c_2 x)$$

with the unknown x and c_1 , c_2 being arbitrary constants has a solution only for

$$(12) \quad c_1 \cdot c_2 < 1/e$$

If Eq.(9) is substituted into (11) this leads with Eq.(12) to the following worst case estimate for the existence of a solution to the oxidation modeling problem:

$$(13) \quad \frac{(1-a)}{a} sg a \mu_0 k_{n0} \frac{V_u - V_c}{kT} < 1/e$$

For low temperatures ($\leq 900^\circ$) no solution exists with parameter values taken from [1]. Thus only Eqs.(1) and (2) were implemented into the 2D simulator.

3.2. Stability of initial value problem

The stability of an initial value problem is assured as long as the eigenvalue $\epsilon^{k+1}/\epsilon^k$ is inside the unit circle of the complex plane. In the case of stress-independent coefficients, the right hand side of (5) is merely a function of the geometry. For this case the stability condition reads:

$$|1 + dt \cdot sg \cdot R_a(a^k)| < 1$$

with $R(a)$ being the right hand side of (5), and R_a its derivative with respect to a . The stability can be assured by an

appropriate choice of the time-step-size dt . If the coefficients are stress-dependent, the growth-rate is not only a function of the radius a but also of its derivative with respect to time a_t which serves as a measure for the oxide flow velocity. For this case Eq.(5) takes the form:

$$a_t = sg R(a, a_t)$$

The explicit time discretization of [1] yields the following recursive formula:

$$a^{k+1} = a^k + dt \cdot sg \cdot R(a^k, \frac{a^k - a^{k-1}}{dt})$$

A linearization enables us to consider the stability conditions in the small signal regime:

$$R_a := \delta R / \delta a \quad \text{und} \quad R_{a_t} := \delta R / \delta a_t$$

The value of the old time-step a^k is now being disturbed by ϵ^k . The resulting error of the new time-step becomes:

$$\epsilon^{k+1} = \epsilon^k (1 + dt \cdot sg \cdot R_a + R_{a_t})$$

Therefore the condition for stability is:

$$|1 + dt \cdot sg \cdot R_a + R_{a_t}| < 1$$

The appearance of a_t within the right hand side of Eq.(5) leads to a term in the expression for the eigenvalue which cannot be influenced by an appropriate choice of dt . Thus instability can only be prevented by a more implicit time-discretization.

3.3. Implementation of model for stress-dependent reaction rate

A fully nonlinear solution of the equation system arising from an implicit time integration using Newton's method would lead to a tremendous increase in computation time. Therefore, in this work, a relatively simple linearization method well-suited for the restricted Kao-model (Eqs.(1) and (2)) is proposed. The displacement of a point on the Si-SiO₂ interface during one time-step is calculated as the product of oxygen-concentration time-step-size and the reaction-rate which is obtained as a function

of the normal-stress according to Eq.(1):

$$(14) \quad d_z = dt C_s k_o \exp(-\sigma_n V_k/kT)$$

A linearization of this expression yields:

$$(15) \quad \frac{\Delta d_z}{\Delta \sigma_n} = - \frac{dt V_k C_s k_o}{k T} \exp(-\sigma_n V_k/kT)$$

with

$$\begin{aligned} \Delta d_z &= d_z - d_{z_o} \quad \text{und} \\ \Delta \sigma_n &= \sigma_n - \sigma_{n_o} \end{aligned}$$

a linear formulation of the boundary condition for the viscous deformation is obtained. The value of σ_n was expressed in terms of a force applied to the boundary nodes. Thus the numerically critical evaluation of normal stress by the first derivative of the displacements was not necessary.

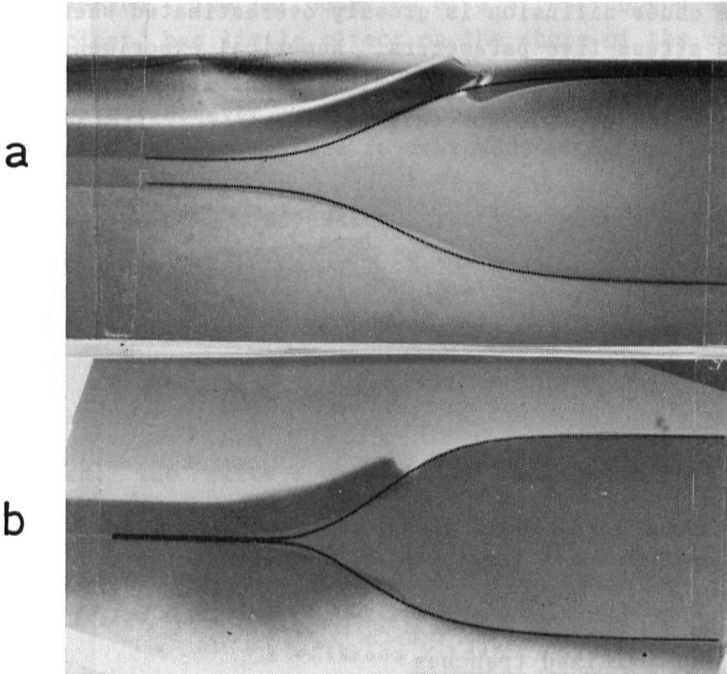


Fig.3: Comparison simulation-measurement for bird's beak with a buffer-oxide-thickness of 800A (a) and 100A (b).

4. COMPARISON SIMULATION - MEASUREMENT

4.1. LOCOS process

First, the results will be discussed for a variation of the buffer-oxide thickness with all other parameters constant. Fig.3a shows good agreement between measurement and simulation for a thick buffer oxide (800Å). For the 100Å buffer oxide (Fig.3b) the experimentally obtained under-diffusion-region is shorter than with the thick buffer-oxide (as expected), but it is still longer and flatter than in the stress-free simulation case. This gives rise to the assumption of increasing stress-effect with decreasing buffer-oxide-thickness.

Fig.4 shows a field oxide structure processed with a very thick nitride mask at 1100°. Direct deformation of the oxide surface by the pressure of the nitride can be observed. In addition, the reduction of the reaction rate at the Si-SiO₂ interface is clearly visible. Fig.5 shows that the effect of a thick nitride mask can be explained by a stress-dependent reaction rate. Good qualitative agreement is achieved with $V_k=25A^3$ (s. Eq.(1)), whereas the under-diffusion is grossly overestimated when calculated with stress-free parameters. Numerical experiments with a variation of V_D did not lead to significant influence on the shape of the oxide profile for this case.

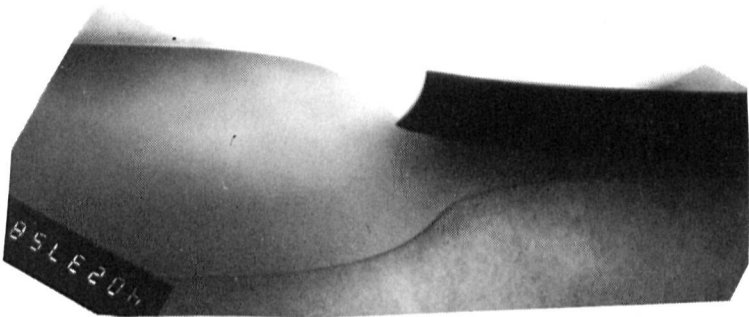


Fig.4: Bird's-beak grown at 1100° with a nitride-mask thickness of 2000Å

4.2 Analysis of oxidized trenches

Fig.6 gives a qualitative impression of the effect of different models for SRO. A rounding of the convex corner is observed in the stress-free calculation (a). The growth rate is reduced at both corners when the stress-dependent reaction rate is taken

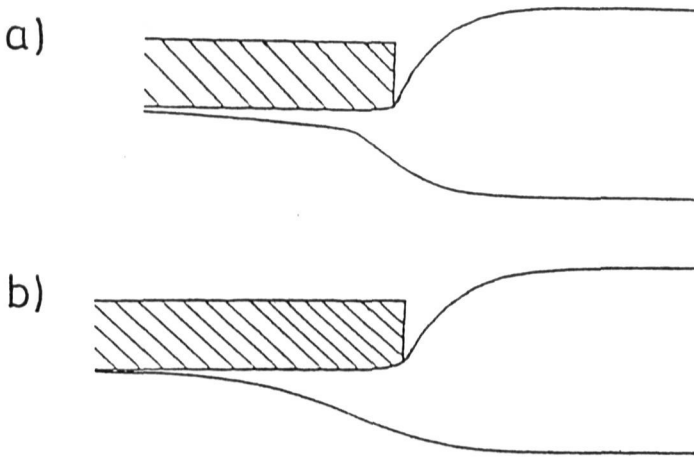


Fig.5: Simulation of local oxidation with stiff nitridemask with stress-dependent coefficient (a), stress-free simulation (b)

into account. The formation of a "horn" at the convex corner can be observed. The introduction of a stress-dependent diffusion coefficient has little effect on the shape of the convex corner (c). It seems that the growth velocity is limited by the reaction rate. However, at the concave corner an additional reduction of the growth rate is achieved.

In the case of a $\langle 100 \rangle$ -Wafer, the vertical walls of a trench with an angle of 0° and 90° to the flat have $\langle 110 \rangle$ orientation. The oxide which covers the walls can be thicker than the oxide covering the wafer surface by a factor up of to 1.5. Thus the introduction of an orientation dependent reaction rate is needed as prerequisite to render satisfactory agreement between measurement and simulation feasible. The following simplified model is proposed. The effective reaction rate is given by the scalar product

$$(16) \quad k_{eff} = n \cdot k \quad \text{with}$$

$$k = (k_{100}, k_{110})^T$$

where n denotes the unit vector normal on the Si-SiO₂ interface and k_{100} , k_{110} the reaction rates for $\langle 100 \rangle$ and $\langle 110 \rangle$ orientation respectively. For the concave corner of the trench the best

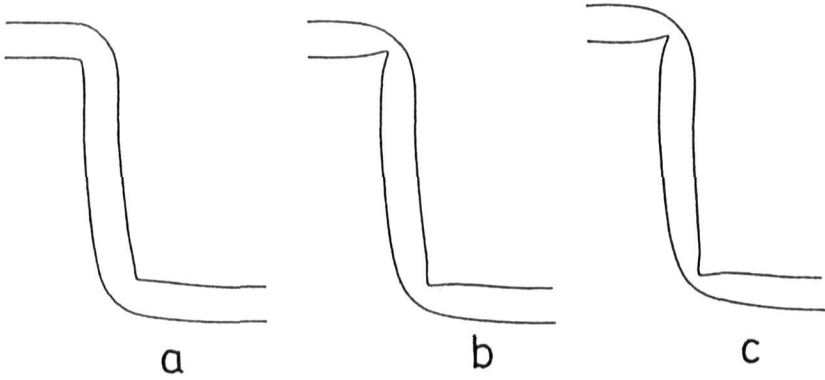


Fig.6: Simulation of oxidation of a step-shaped silicon structure. Stress-free model (a), $V_k=25Aa^3$ (b), $V_k=V_D=25A^3$ (c)

fit shown by Fig.7 was obtained with $V_k=V_D=25A^3$. This turned out to be more difficult at the convex corner. The stress-effect was grossly over-estimated (Fig.8). The reason for this problem is the very small radius of curvature of the convex corner. In the case of the rotational symmetric model according to Eq.(7) and Eq.(8), indefinite values for normal stress and pressure are obtained. The experimental results indicate that in regions with extreme tension an additional mechanism is present which acts as a limitation to stress. This could be modelled in terms of a stress-dependent viscosity similar to Kao's proposal according to Eq.(4) or by assuming a plastic mechanism for deformation.

5. CONCLUSION

Numerical stability and the existence of a solution was checked for the case that Kao's model for SRO is included into a 2-D simulator. A proposal for efficient numerical realization of this model within a simulation program is given. It was shown that the dominant stress-effects can be explained by the stress-dependence of the reaction rate for LOCOS process. Improvement of the models is needed to describe the oxidation behaviour at sharp corners.

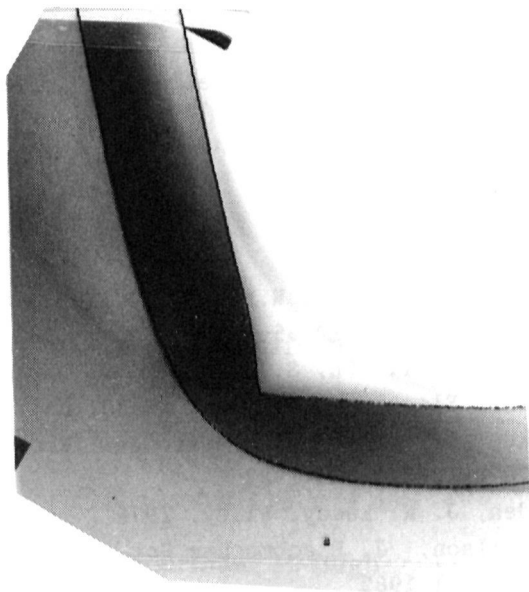


Fig.7: Concave corner of oxidized trench: comparison of simulation and measurement

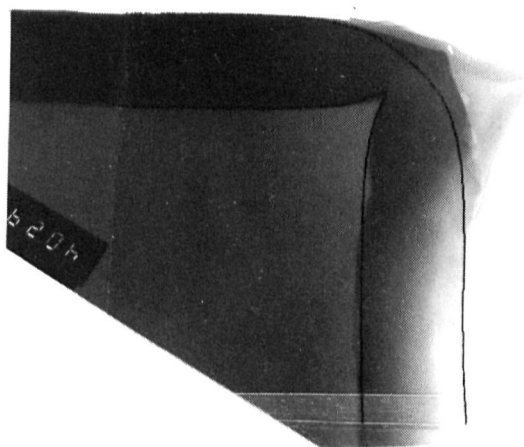


Fig.8: Comparison simulation-measurement of convex corner of oxidized trench.

ACKNOWLEDGEMENTS

The authors wish to thank Prof. S. Selberherr for valuable advice and helpful discussions.

REFERENCES

- [1] D.B.Kao, J.P.McVittie, W.D.Nix, K.C.Saraswat, IEEE Trans. Electron Dev., Vol. ED-35, No. 1, Jan. 1988
- [2] D. Chin, S. Y. Oh, S. M. Hu, R. W. Dutton, J. L. Moll, IEEE Trans. Electron Dev., Vol. ED-30, Jul. 1983
- [3] R.B.Markus, T.T.Sheng, J. Electrochem. Soc., Vol. 129, No. 6, pp. 1278-1282, Juni 1982
- [4] J. T. Oden, J. N. Reddy, Wiley, 1976
- [5] L. O. Wilson, J. Electrochem Soc., Vol. 129, No. 4, pp. 831-837, April 1982
- [6] K. Yoshikawa, Y. Nagakubo, K. Kanyaki, Extended Abstracts of the 16th IEDM, Kobe, 1984, pp. 475-478
- [7] A. Poncet, IEEE Trans. CAD, vol. CAD-4, No. 1, Jan 1985, pp. 41-53
- [8] P.Sutardja, W.G.Oldham, IEDM'86, Los Angeles, Dec. 7-10. 1986